

X-RAY COUNTERPARTS OF TEV SOURCES NEWLY DISCOVERED WITH H.E.S.S.

E. Ferrero, S. Wagner, G. Pühlhofer, and the H.E.S.S. collaboration

Landessternwarte Heidelberg, Königstuhl 12, D-69117, Heidelberg, Germany

ABSTRACT

The High Energy Stereoscopic System (H.E.S.S.) is a second generation array of four Imaging Cherenkov Atmospheric Telescopes situated in Namibia, with unprecedented sensitivity compared to past gamma-ray experiments. H.E.S.S. has tripled the number of Galactic sources detected at TeV energies. Some of them do not have a firm identification yet. The search for possible counterparts at other wavelengths is fundamental for both a correct identification and a physical description of the new TeV sources. Here we present the new Galactic sources detected by H.E.S.S. during its first year of operations and we discuss their possible X-ray counterparts.

Key words: Gamma-rays; supernova remnants; pulsar wind nebulae.

1. INTRODUCTION

The study of astrophysical sources above $\sim 10^{11}$ eV, in the TeV range ($1 \text{ TeV} = 10^{12}$ eV), is the domain of Very High Energy (VHE) astronomy. At these energies, the most effective way to detect gamma-rays is on the ground, through the Imaging Atmospheric Cherenkov Technique. This method is based on the detection of the Cherenkov light emitted by showers of secondary particles generated by the interaction of a primary gamma-ray with the molecules of the upper atmosphere (see Fig. 1). The use of several telescopes provides a multiple view of the same shower and allows to reconstruct the photon's direction with good precision. The big advantage of such a technique is the large collecting area of $\sim 10^5 \text{ m}^2$ at 1 TeV. As a comparison, gamma-ray satellites have typical detection areas of the order of square metres, too small to be able to collect a sufficiently large number of VHE photons given their very low flux. For this reason VHE astronomy in space remains unpractical at present.

The main goals of VHE astronomy, for the purposes of these proceedings, are the identification of the sites of particle acceleration and of the acceleration mechanisms, as well as the determination of the nature of the emitting particles (hadrons or leptons). VHE photons are ex-

pected to be produced at the sites where particles are accelerated up to TeV energies by different possible mechanisms: decay of neutral pions produced in hadronic interactions, Inverse Compton scattering of electrons, non-thermal bremsstrahlung and synchrotron emission from ultra-high energy particles. Therefore VHE photons can be used as tracers of the acceleration sites because, as opposed to the particles, they are not affected by magnetic fields and they retain directional information.

The High Energy Stereoscopic System (H.E.S.S.) is a TeV instrument situated in the Khomas Highlands in Namibia at an altitude of 1800 m. It consists of a square array of four Imaging Atmospheric Cherenkov Telescopes (IACTs) with a side length of 120 m, a value chosen to maximize the sensitivity above ~ 100 GeV. Each telescope has a mirror area of $\sim 107 \text{ m}^2$ and is equipped with a camera constituted by 960 fast photomultiplier tubes. H.E.S.S. is sensitive to the energy range from ~ 100 GeV up to a few tens TeV. The large field of view of 5° is especially suited for the study of extended sources and for surveys. The angular resolution is of the order of a few arcminutes. The sensitivity is about an order of magnitude higher than that of previous TeV instruments and reaches 1% of the Crab flux for a 5σ detection in 25 hours. H.E.S.S. works in stereoscopic mode, meaning that a photon is recorded only when at least two telescopes are triggered at the same time, which allows a considerable reduction of hadronic background. The system has been fully operational since January 2004. For more information about H.E.S.S. see for example Hinton (2004).

2. THE NEW H.E.S.S. GALACTIC SOURCES

Galactic TeV astronomy before the beginning of H.E.S.S. activities was limited to a handful of objects (see e.g. Weekes 2003). Among these, only a few were detected by more than one instrument and were considered as firm sources, whereas the majority was still waiting for independent confirmations. After about one year of observations with the full H.E.S.S. array the situation has dramatically changed. Table 1 lists all the Galactic sources detected by H.E.S.S. up to September 2005. Some of them are well known sources, previously detected at TeV ener-

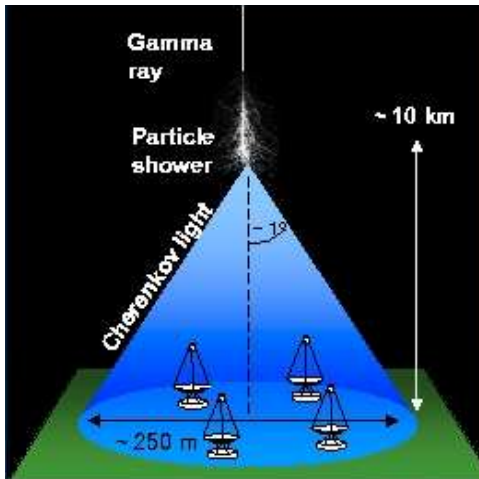


Figure 1. Sketch of the Imaging Atmospheric Cherenkov Technique as implemented by H.E.S.S.

gies by other instruments, but the majority have been discovered during a survey of the inner part of the Galactic Plane (Aharonian et al. 2005a, Aharonian et al. 2005b). One should note that some earlier claimed TeV sources (SN 1006 and PSR 1706-44) could not be confirmed by H.E.S.S. and thus are not included in Table 1. Only upper limits could be determined for these sources and the results are reported elsewhere (Aharonian et al. 2005c, Aharonian et al. 2005d).

At present, there are twenty-four H.E.S.S. Galactic sources, but this number will very likely increase in the near future. All the sources are detected above a 4σ significance level (post-trials, i.e. accounting for the number of grid points in the sky map tested for the presence of a source) and most of them appear to be considerably extended. The Galactic latitudes of the sources (Table 1, Col. 3) show that all of them cluster along the Galactic Plane. Typical systematic errors on the photon fluxes listed in Table 1 are of the order of 30%.

3. X-RAY COUNTERPARTS

Given the above results a search for possible counterparts of the new Galactic sources has been undertaken. Since gamma-ray instruments in the MeV-GeV ranges, like e.g. EGRET, do not allow to establish firm associations with the H.E.S.S. sources due to their poor angular resolutions, the most natural band where one would look for counterparts of TeV sources is the X-ray band. Based on their X-ray counterparts we have qualitatively divided the TeV sources into four groups (see Table 1). The first one includes the firm X-ray/TeV associations; as an example, in this group we find the two shell-like SNRs RX J1713.7-3946 and Vela Junior (RX J0852.0-4622). Their TeV emission is spatially well resolved and reveals a shell structure which correlates very well with that seen in the X-ray band (Aharonian et al. 2004, Aharonian et al. 2005e). In the second group we have the likely

associations, such as, for example, the plerion of the pulsar PSR J1826-1334 (see Fig. 4). For this object the association is based on both spectral arguments and considerations on the relative extents and positions of the X-ray and TeV emission regions (Aharonian et al. 2005f), although in this case we do not see highly spatially correlated morphologies as in the two SNRs discussed above. In the third group we have placed sources for which a good positional coincidence is found between the TeV emission and an X-ray source, but for which no other strong argument exists in favour of the association. Some of these sources might eventually turn out to be spurious identifications. The fourth group includes all the sources for which no X-ray counterpart has been found so far. For some of the sources (“dark” sources) no counterpart could be found at any wavelength. However, it is not clear yet whether the absence of X-ray counterparts is due to an intrinsic X-ray weakness of the sources or just to the lack of X-ray observations covering their entire TeV emission regions. Deeper investigations on these objects are under way.

We will consider from now on only the first two groups of reliable associations and we will show some examples in more detail. As the majority are plerions, in the following we will concentrate mainly on these sources. However, for completeness, we will also show the case of the shell-like SNR RX J1713.7-3946, which is a beautiful example of the imaging capabilities of H.E.S.S.

Vela X. Figure 2 shows a smoothed excess map of the Vela X region with ROSAT contours overlaid on it. The TeV emission of HESS J0834-456 is clearly elongated and extends to the south-west of the Vela pulsar (Khélifi et al. 2005). It overlaps very well with the X-ray emission as seen by ROSAT, which is believed to originate from a pulsar jet (Markwardt & Ögelman 1995). The analysis of this source is still in progress (Aharonian et al. 2005g, in preparation).

MSH 15-52. Figure 3 shows a smoothed excess map of the SNR MSH 15-52 as well as ROSAT contours from Trussoni et al. (1996). The centroid of the TeV emission is indicated by the black star on the left, whereas the pulsar’s position is given by the black dot on the right. As one can see the TeV excess is significantly extended and roughly centered on the pulsar’s location. The TeV emission region is well compatible with the extension of the X-ray emission from a diffuse PWN surrounding the pulsar. This represents the first resolved image of a PWN at TeV energies (see also Aharonian et al. 2005h).

HESS J1825-137. Figure 4 is an unsmoothed excess map of the PWN associated with the Vela-like pulsar PSR J1826-1334. Also shown in the figure are the XMM contours, the 95% confidence region of a closeby unidentified EGRET source which might be associated with the H.E.S.S. source, the best fit position of the TeV excess and its best fit size (see caption of Figure 4). The X-ray emission is asymmetric with respect to the pulsar’s posi-

Table 1. List of Galactic sources detected by H.E.S.S. during its first year of operations. Col. 1: H.E.S.S. name; Col. 2: Galactic longitude; Col. 3: Galactic latitude; Col. 4: photon flux above the threshold energy shown in parentheses; Col. 5: counterpart, or possible counterpart (in italic); Col. 6: type of counterpart; Col. 7: division of the sources into different groups according to their X-ray counterparts.

H.E.S.S. Name	l (°)	b (°)	$F_{\text{ph}}(> E_{\text{TeV}})$ ($10^{-12} \text{ cm}^{-2} \text{ s}^{-1}$)	Possible counterpart	Type	Group
J1713-397	347.28	-0.38	14.6(>1)	RX J1713.7-3946	SNR shell	
-	266.28	-1.24	19.0(>1)	Vela Junior	SNR shell	
J0834-456	263.86	-3.07	14.5(>1)	Vela X	plerion	Firm X-TeV
J1514-591	320.33	-1.19	22.6(>0.28)	MSH 15-52	plerion	associations
-	304.19	-0.99	<2-6(>0.38)	PSR B1259-63	“binary plerion”	
-	-5.78	19.1(>1)	Crab	plerion		
J1747-281	0.87	0.08	5.5(>0.2)	G 0.9+0.1	plerion	
J1745-290	359.95	-0.05	18.2(>0.17)	Gal. Center	BH/SNR?	
J1826-148	16.90	-1.28	5.1(>0.25)	LS 5039	Microquasar	Likely X-TeV
J1825-137	17.82	-0.74	39.4(>0.2)	PSR J1826-1334	plerion	associations
J1813-178	12.81	-0.03	14.2(>0.2)	G 12.82	SNR shell/PWN	
J1837-069	25.18	-0.11	30.4(>0.2)	<i>G 25.5+0.0</i>	SNR/PWN?	
J1713-381	348.65	0.38	4.2(>0.2)	<i>CTB 37B</i>	SNR?	
J1640-465	338.32	-0.02	20.9(>0.2)	<i>G 338.3-0.0</i>	SNR	X-TeV positional
J1634-472	337.11	0.22	13.4(>0.2)	<i>IGR J16358-4726?</i>	Unid.	coincidences
J1632-478	336.38	0.19	28.7(>0.2)	<i>IGR J16320-4751?</i>	Unid.	
J1804-216	8.40	-0.03	53.2(>0.2)	<i>G 8.7-0.1</i>	SNR/PWN?	
J1303-631	304.23	-0.36	12.0(>0.38)	-	“Dark”	
J1834-087	23.24	-0.32	18.7(>0.2)	<i>G 23.3-0.3</i>	SNR	
J1745-303	358.71	-0.64	11.2(>0.2)	<i>3EG 1744-3011</i>	Unid.	No X-rays
J1708-410	345.67	-0.44	8.8(>0.2)	-	“Dark”	
J1702-420	344.26	-0.22	15.9(>0.2)	-	“Dark”	
J1616-508	332.39	-0.14	43.3(>0.2)	<i>PSR J1617-5055</i>	PWN?	
J1614-518	331.52	-0.58	57.8(>0.2)	-	“Dark”	

tion, extending towards the south. It has been attributed to synchrotron emission from a PWN (Gaensler et al. 2003). The TeV emission extends further to the south and covers a larger area with respect to the X-rays. Aharonian et al. (2005f) argue that this emission is also associated with the PWN by interpreting both the offsets of the emission regions observed in the X-ray and TeV bands and the corresponding spectra in terms of longer lifetimes of the TeV emitting electrons compared to those of the X-ray electrons.

RX J1713.7-3946. This is a well-known shell-like SNR. Figure 5 shows a smoothed excess map with ASCA contours (1-3 keV) overlaid on it. The TeV emission clearly shows a shell morphology which traces very well that observed in the X-ray band (Aharonian et al. 2004). The quality of the TeV image is such that it allows to perform, for the first time at these energies, a spatially resolved spectral analysis (Aharonian et al. 2005i, submitted).

4. PROPERTIES OF THE SOURCES

The increasing number of newly discovered TeV sources allows for the first time to carry out population studies at very high energies. It is now possible to start to answer questions such as whether the TeV spectra are correlated in any way with those in the X-ray band or in other bands, or with any other properties of the objects. The aim of these studies is eventually to understand the physics behind particle acceleration and this requires a multiwavelength approach. As an initial attempt in this direction in Table 2 we have summarized the TeV results and the X-ray data from the literature for the plerions for which a reliable association between the emission in the two bands has been established (i.e. first two groups in Table 1). Basically all of the sources show X-ray and TeV photon indices falling in the range 2-3, with the exception of the rather flat Γ_X of PSR B1259-63. This is, however, a rather peculiar system with a pulsar orbiting a massive Be star and interacting periodically with the companion’s

Table 2. X-ray and TeV data for plerions with a reliable association between the X-ray and TeV emission. Col. 1: name of the source; Col. 2 and 3: monochromatic fluxes at 1 TeV and 1 keV, respectively; Col. 4: ratio of these two fluxes; Col. 5 and 6: gamma-ray and X-ray photon indices; Col. 7: age of the source.

Source	$F_{1 \text{ TeV}}$ ($10^{-12} \text{ erg s}^{-1} \text{ cm}^{-2} \text{ TeV}^{-1}$)	$F_{1 \text{ keV}}$ ($10^{-12} \text{ erg s}^{-1} \text{ cm}^{-2} \text{ keV}^{-1}$)	$F_{1 \text{ TeV}}/F_{1 \text{ keV}}$ (10^{-10})	Γ_{TeV}	Γ_{X}	Age (yrs)
Vela X	21.55	234.44	0.92	1.90	2.4	11000
MSH 15-52	9.12	11.27	8.09	2.27	2.05	~ 1700
PSR B1259-63	2.08	8.48	2.45	2.70	1.7	3×10^5
Crab	49.76	14352.0	0.03	2.63	2.11	951
G 0.9+0.1	1.35	5.78	23.36	2.40	1.99	~ 1000
HESS J1825-137	9.43	0.72	1.31	2.40	2.30	21000

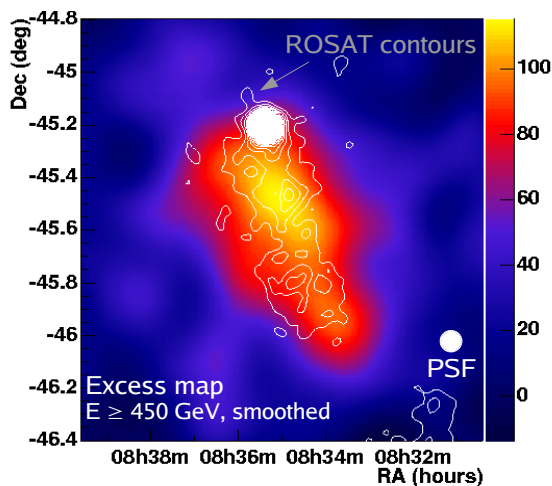


Figure 2. Smoothed excess map of Vela X with ROSAT contours (0.9-2.0 keV) from Marquardt & Ögelman (1995).

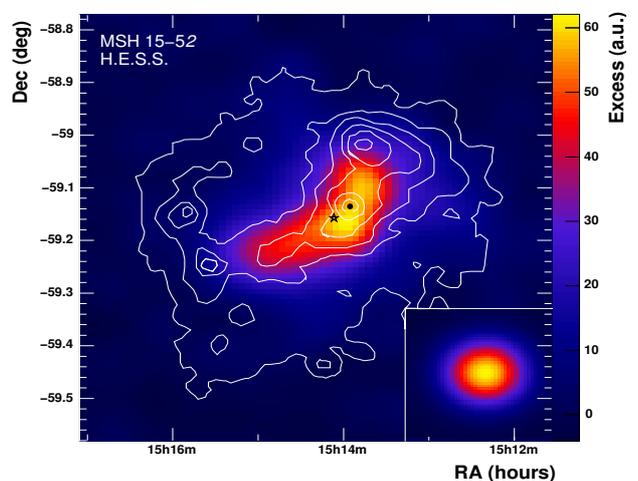


Figure 3. Smoothed excess map of the SNR MSH 15-52 with ROSAT contours (0.6-2.1 keV) from Trussoni et al. (1996).

disk wind (Aharonian et al. 20051). Nevertheless, one must be aware that these photon indices represent spatial averages over extended sources (time averages in the case of PSR B1259-63).

The gamma – to – X-ray flux ratio spans a rather wide range of about three orders of magnitude. This might be explained by the dependence on the square of the magnetic field which can vary considerably from source to source.

Overall no trivial correlation can be found between any of the quantities listed in Table 2. However, before drawing any general conclusions and before addressing the issue of particle acceleration physics, one should make sure to explore the entire multiwavelength parameter space of the sources. Accordingly, the present effort is to collect multiwavelength data for all of these sources, through the use of both new and archival observations, in order to be able to answer these questions. Special attention is given to the “dark” sources in an attempt to understand whether they might belong to new classes of particle accelerators or whether, more simply, they might be previously unde-

tected PWN/SNRs. To this purpose we have been granted XMM and Chandra observing time for a sample of new Galactic TeV sources and the analysis of the data is under way.

5. CONCLUSIONS

We have presented the new Galactic TeV sources discovered by H.E.S.S. during its first year of operations. With respect to previous years the number of this sources has tripled and the search for counterparts at other wavelengths is in progress. Two SNR (RX J1713.7-3946 and Vela Junior) show a shell morphology at TeV energies which correlate spatially very well with the X-ray structure, proving the unprecedented imaging capabilities of H.E.S.S. at very high energies. The majority of the sources with a reliable X-ray identification are plerions and some examples have been presented in more detail. The large number of sources allows for the first time

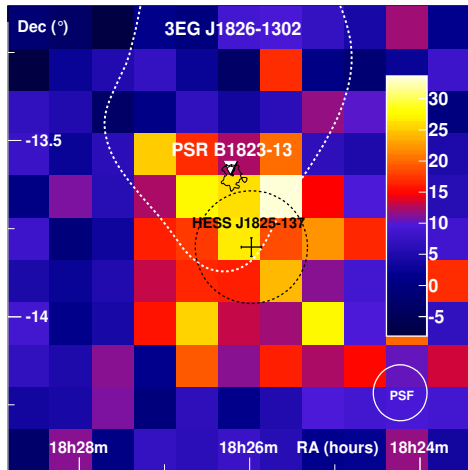


Figure 4. Unsmoothed excess map of HESS J1825-137 with XMM contours (black) from Gaensler et al. (2003). Also shown are the 95% confidence region of a closely unidentified EGRET source (dotted white line), the best fit position of the TeV source (cross) and its best fit size (dotted black circle).

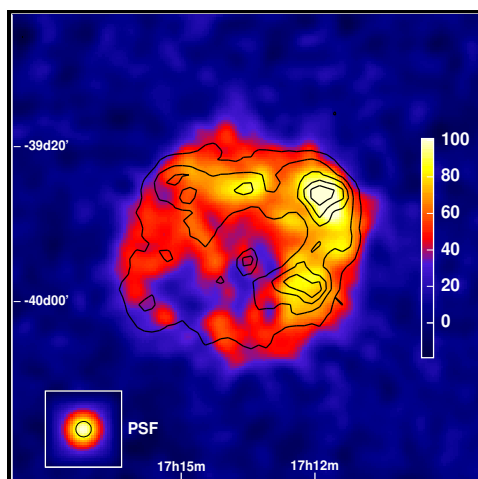


Figure 5. Smoothed excess map of RX J1713.7-3946 with ASCA contours (1-3 keV).

to study the properties of different classes of objects, although definite conclusions have to wait for the results of deeper multiwavelength investigations currently under way.

REFERENCES

- Aharonian, F., et al. (H.E.S.S. collaboration) 2005a, *Science*, 307, 1938
- Aharonian, F., et al. (H.E.S.S. collaboration) 2005b, *ApJ*, in press, astro-ph/0510397
- Aharonian, F., et al. (H.E.S.S. collaboration) 2005c, *A&A*, 437, 135
- Aharonian, F., et al. (H.E.S.S. collaboration) 2005d, *A&A*, 432, 9
- Aharonian, F., et al. (H.E.S.S. collaboration) 2005e, *A&A*, 437, 7
- Aharonian, F., et al. (H.E.S.S. collaboration) 2005f, in press, astro-ph/0510394
- Aharonian, F., et al. (H.E.S.S. collaboration) 2005g, in preparation
- Aharonian, F., et al. (H.E.S.S. collaboration) 2005h, *A&A*, 435, 17
- Aharonian, F., et al. (H.E.S.S. collaboration) 2005i, *A&A*, submitted
- Aharonian, F., et al. (H.E.S.S. collaboration) 2005l, *A&A*, 442, 1
- Aharonian, F., et al. (H.E.S.S. collaboration) 2004, *Nature*, 432, 75
- Gaensler, B.M., Schulz, N.S., Kaspi, V.M. et al. 2003, *ApJ*, 588, 441
- Hinton, J.A. (H.E.S.S. collaboration) 2004, *New Astronomy Review*, 48, 331
- Khélifi, B., et al. (H.E.S.S. collaboration) 2005, *Proc. 29th ICRC (Pune 2005)*, <http://icrc2005.tifr.res.in/html/PAPERS/OG22/ger-khelifi-B-abs1-og22-oral.pdf>
- Markwardt, C.B. & Ögelman, H. 1995, *Nature*, 375, 40
- Trussoni, E., Massaglia, S., Caucino, S., et al. 1996, *A&A*, 306, 581
- Weekes, T.C. 2003, *Proc. 28th ICRC (Tsukuba 2003)*, Universal Academy Press, 5, 2875